Published in final edited form as:
J Comp Neurol. 2002 February 11; 443(3): 259–274. doi:10.1002/cne.10117.

A Quantitative Morphometric Analysis of Rat Spinal Cord Remyelination Following Transplantation of Allogenic Schwann Cells

KAREN L. LANKFORD, **TOSHIO IMAIZUMI**, **OSAMU HONMOU**, and **JEFFERY D. KOCSIS***
Department of Neurology, Yale University School of Medicine, PVA/EPVA Neuroscience Regeneration Research Center, and Rehabilitation Research and Development Center, VA Medical Center, West Haven, Connecticut, 06516

Abstract

Quantitative morphometric techniques were used to assess the extent and pattern of remyelination produced by transplanting allogenic Schwann cells into demyelinated lesions in adult rat spinal cords. The effects of donor age, prior culturing of donor cells, prior lesioning of donor nerves, and host immunosuppression were evaluated by transplanting suspensions of 30,000 acutely dissociated or cultured Schwann cells from neonatal, young adult, or aged adult rat sciatic nerves into X-irradiation and ethidium bromide-induced demyelinated dorsal column lesions, with or without co-transplantation of neonatal optic nerve astrocytes. Three weeks after transplantation, spinal cords were processed for histological analysis. Under all Schwann cell transplant protocols, large areas containing many Schwann cell-like myelinated axon profiles could be readily observed throughout most of the lesion length. Within these "myelin-rich" regions, the vast majority of detectable axons showed a peripheral-like pattern of myelination. However, interaxonal spacing also increased, resulting in densities of myelinated axons that were more similar to peripheral nerve than intact dorsal columns. Freshly isolated Schwann cells remyelinated more axonal length than cultured Schwann cells, and cells from younger donors remyelinated slightly more axon length than cells from older donors, but all Schwann cell transplant protocols remyelinated tens of thousands of millimeters of axon length and remyelinated axons at similar densities. These results indicate that Schwann cells prepared under a variety of conditions are capable of eliciting remyelination, but that the density of remyelinated axons is much lower than the myelinated axon density in intact spinal cords.

Indexing terms

cell transplantation; cell therapy

Transplantation of myelin-forming cells into demyelinated lesions has long been considered as a potential therapy for patients with demyelinating diseases or some types of CNS injuries. Numerous studies using a variety of donor cell types and tissues have demonstrated the ability of transplanted myelin-forming cells to myelinate demyelinated CNS axons (Blakemore, 1977; Duncan et al., 1981; Gumpel et al., 1983, 1987; Blakemore et al., 1987; Trotter et al., 1993; Franklin et al., 1995; Honomu et al., 1996, Barnett et al., 2000; Kato et al., 2000). Electrophysiological studies have further demonstrated that spontaneous invasion of Schwann cells into a lesion (Blight and Young, 1989; Felts and Smith, 1992), as well as transplantation of Schwann cells (Honmou et al., 1996) or olfactory ensheathing cells (OECs; Imiazumi et al.,

*Correspondence to: Jeffery D. Kocsis, Ph.D., Yale University School of Medicine, Neuroscience Research Center (127A), Department of Veterans Affairs Medical Center, West Haven, CT 06516., E-mail: jeffery.kocsis@yale.edu.

1998) into chemically demyelinated lesions can improve impulse conduction across the lesion. The paucity of detailed quantitative data on the extent of remyelination resulting from transplantation of myelin-forming cells, however, has made it difficult to compare the effectiveness of different transplant protocols or to assess the overall feasibility of cell therapies as a treatment strategy (for review, see Duncan and Milward, 1995).

Schwann cells have been considered by many investigators to be strong candidates for remyelinating cell therapies. Although Schwann cells are normally excluded from the CNS during development, they spontaneously invade the CNS and remyelinate CNS axons under numerous pathological conditions including multiple sclerosis (Feigin and Popoff, 1966; Feigin and Ogata, 1971; Ghatak et al., 1973; Ogata and Feigin, 1975; Prineas and Collenil, 1979; Itoyama et al., 1983, 1985; Rodriguez, 1992; Prineas et al., 1993) and CNS trauma (Hughes and Brownel, 1963; Harrison and McDonald, 1977; Griffiths and McCulloch, 1983; Perry and Hayes, 1985; Blight and Young, 1989; see also Franklin and Blakemore, 1993 and Baron-van Evercooren, 1997 for reviews). Because Schwann cells express different surface antigens than oligodendrocytes (Mirsky et al., 1980; Raisman et al., 1993) and are spared autoimmune attack in patients with multiple sclerosis (MS), they might also be able to serve as permanent replacements for oligodendrocytes in MS lesions. Schwann cells are also more readily accessible than either oligodendrocytes or OECs and would therefore be easier to obtain directly from the patient, thereby avoiding the need for immunosuppression.

Much data suggest that resident astrocytes in demyelinated lesions can pose a barrier to Schwann cell migration (Franklin et al., 1992; Blakemore et al., 1995; Iwashita et al., 2000; for an overview, see also Blakemore and Franklin, 2000 and Franklin and Blakemore, 1993). However, other results imply that astrocytes do not always pose an absolute barrier to Schwann cells. For example, native Schwann cells have been shown to migrate into and myelinate axons within the penumbra of electrolytic lesions that kill oligodendrocytes but spare axons and astrocytes (Li et al., 1999). Transplanted Schwann cells have also been reported to migrate considerable distances from injection sites in the intact rat hippocampus (Brook et al., 1993; Raisman et al., 1993) or thalamus (Brook et al., 1994), despite an astrocytic hypertrophy (Raisman et al., 1993). Moreover, the transplantation of Schwann cells into newborn myelin-deficient (md) rats, which show a marked astrogliosis, results in significant myelination (Duncan et al., 1988), and Schwann cells have been shown to migrate up to 8 mm within the CNS of dysmyelinating Shiverer mutant mice (Baron-Van Evercooren et al., 1992, 1993).

In this study we transplanted rat sciatic nerve Schwann cells into X-irradiated and ethidium bromide-injected demyelinated lesions in the rat dorsal funiculus and used quantitative morphometric methods to compare the extent and pattern of remyelination resulting from different transplant protocols. Donor cell ages, prior cell history, the presence or absence of co-transplanted astrocytes, and immunological state of the host were each independently varied in order to evaluate the importance of each parameter for successful remyelination. We did not attempt to investigate the influences of the native glial environment in promoting or inhibiting transplant-induced remyelination or to compare the repair efficiency of different types of myelin-forming cells, but instead focused on evaluating the repair potential of Schwann cells transplanted into a demyelinated lesion model depleted of both astrocytes and oligodendrocytes. Although we cannot directly extrapolate these results to astrocyte-rich demyelinated lesion, such as those in demyelinating diseases, the results provide potentially useful information on the influence of donor age and cell preparation protocols on the remyelinating potential of Schwann cells.

MATERIALS AND METHODS

Induction of demyelinating lesions

The experiments were conducted with approval from the Yale University Institutional Animal Care and Use Committee. Adult female Wistar rats were subjected to a standard lumbar spinal cord X-irradiation and ethidium bromide injection (X-EB) protocol, described in detail in Honmou et al. (1996). Briefly, rats were anesthetized with ketamine (75 mg/kg) and xylazine (10 mg/kg) and X-irradiated utilizing Siemens (South Iselin, NJ) Stabilipan radiotherapy to deliver a 40 Gy surface dose of X-irradiation through a 2 × 4-cm opening in a 4-mm-thick lead shield in the area of the spinal cord caudal to T-10. Three days after irradiation, a sterile laminectomy was performed under anesthesia, and demyelinating lesions were induced by injecting a total of 3 μl of 0.3 mg/ml ethidium bromide into the dorsal funiculus (often generically referred to as the dorsal column) via a drawn glass micropipette. Three pairs of injections of 0.5 μl each were made at 2-mm intervals along the length of the spinal cord at depths of 0.7 and 0.4 mm.

Donor cell isolation and culturing

Donor Schwann cells were isolated enzymatically from sciatic nerves of 1 week postnatal (P7) pups, 140 –180-g young adults, or 18-month-old aged adult Wistar or Sprague-Dawley rats. No differences were noted in any aspect of remyelination using donors from these two closely related strains. Schwann cells from P7 neonatal rat sciatic nerves were dissociated by mechanical trituration following a 30-minute incubation with 2.5 mg/ml trypsin (Boehringer Manheim, Mannheim, Germany) in calcium-free complete saline solution (CSS) as described in Brockes et al. (1979). Adult sciatic nerves were desheathed, minced, incubated for 45 minutes in Dulbecco's modified Eagle's medium (DMEM; Gibco BRL, Grand Island, NY) with 10 mg/ml each collagenase A + collagenase D (Boehringer Mannheim), pelleted, incubated for an additional 15 minutes in CSS with 2.5 mg/ml trypsin, and triturated though a fire-polished siliconized pasture pipette. Schwann cells were washed twice with DMEM + 10% fetal bovine serum before plating, and an additional 3 times in DMEM only before transplantation. Cultured Schwann cells were plated on laminin-coated culture flasks and maintained continuously in 70% DMEM, 20% astrocyte-conditioned media, 10% fetal bovine serum, 250 μg/ml bovine pituitary extract (Gibco BRL), and 100 U/ml penicillin + 100 μg/ml streptomycin (Gibco BRL). (When the source of a reagent is unspecified, it is from Sigma, St. Louis, MO.) Note that the source of enzymes was very important to the viability of adult Schwann cells but less so for neonatal cells.

Optic nerve astrocytes were harvested from P3 Wistar rat pups, dissociated with papaine (Worthington, Lake-wood, NJ), and cultured in 10% fetal calf serum in DMEM as described in McCarthy and de Vellis (1980) and Honmou et al. (1996). Astrocyte-conditioned media were collected every 2 days after cells achieved confluence, and cells were harvested for transplantation 1–4 weeks after plating.

Donor cell transplantation

Three days after ethidium bromide injections, the laminectomy site was reopened, and a single site at the center of each lesion was injected with DMEM only, or a suspension of 3×10^4 rat Schwann cells alone, or 2×10^4 optic nerve astrocytes, or 3×10^4 rat Schwann cells + 2×10^4 optic nerve astrocytes. Culture media or cell suspensions were injected via glass micropipetts in volumes of 0.5 μl each at two depths of 0.7 and 0.4 mm, for a total of 1 μl of cell suspension or media transplanted into each lesion. Transplant sites were marked with sterile charcoal to facilitate subsequent identification. Both freshly isolated and cultured Schwann cells were tested as donor sources for rats in each age category. Eight Schwann cell transplanted rats also received daily i.p. injections of 10 mg/kg/day cyclosporin (Sandoz, East Hanover,

NJ), beginning 1 day prior to cell transplantation to test the effect of immunosupression on remyelination.

Tissue processing

Three weeks after transplantation, rats were sacrificed under sodium pentobarbital anesthesia (60 mg/kg i.p.) and perfused with 2% paraformaldehyde + 2% glutaraldehyde (weight/volume in 0.14 M Sorensen's phosphate buffer, pH 7.3). Spinal cords were excised, stored overnight in fixative, cut into 2-mm segments, notched to indicate orientation, post-fixed with 1% osmium (Polysciences, Warrington, PA) for 4 hours, and dehydrated and embedded in Epox-812 (Ernest F. Fullam, Latham, NY), using standard plastic embedding protocols. Alternatively, the spinal cords of some animals (roughly one-third of the total) were removed under deep anesthesia and fixed subsequent to electrophysiological recordings. Ultramicrotome sections (1 μm) were collected every 0.25 mm along the length of the cord and counterstained with methylene blue and azure II (0.5% each in 0.5% borax). Two intact control spinal cords and one sciatic nerve were also processed in the same manner to assess normal dorsal column volume and typical myelinated axon densities of central and peripheral sensory axons.

Histological analysis

To assess both the extent of X-EB-induced demyelination and the amount of remyelination resulting from each transplantation protocol, cross-sectional areas of the medial aspect of the dorsal column or dorsal funiculus within each section, in the demyelinated region any "myelin-rich" areas were first measured using a Nikon microphot microscope with a 4× lens coupled to a MCI CCD2 video camera and interfaced to an Image 1 processing system. Regions showing different degrees of myelination are readily apparent at this magnification by their staining density (see Figs. 1–3). Percentages of target regions that were demyelinated and sizes of areas within the lesion showing relatively high and low levels of presumptive remyelinated axons were then calculated. In some cases, demyelinated areas extended outside the targeted dorsal funiculus region to encompass portions of the lateral aspects of the dorsal column or the ventral horn, yielding values greater than 100% of the targeted area lesioned. Myelinated axons were counted at 100× in 3–10 representative fields in the "myelin-rich" (i.e., remyelinated) and "myelin-poor" (i.e., demyelinated and unremyelinated) regions of the lesion, with the numbers of fields counted depending on the size and heterogeneity of the region.

Total remyelinated axon lengths were calculated by multiplying average remyelinated axon densities in myelin-rich and myelin-poor regions of lesions by their respective cross-sectional areas and integrating across distance (see formulas below).

The reliability of quantitative methods was validated by repeating lesion size measurements and axon counts in selected sections after 3–7 days. Duplicate myelinated axon counts differed by no more than 2% for any myelin-rich or myelin-poor region examined, and total remyelination estimates differed by no more than 4% for any section. Intertest reliability for nonmyelinated axon counts was much lower, and therefore such counts were not used to estimate percentages of myelin restoration.

Dorsal column volumes in lesioned regions of spinal cords and gross lesion sizes were calculated by integrating cross-sectional area measurements across distance. Expected dorsal column volumes were obtained by averaging cross-sectional areas of dorsal columns immediately rostral and caudal to the lesion and multiplying by the distance between these two points and by an empirically derived constant (1.0977). This constant represented the average ratio between dorsal column volumes calculated using cross-sectional areas measured every 0.25 mm and values calculated using the two endpoints only for 12 different pairs of estimates,

and it was used to compensate for the slight expansion of the intact dorsal column in this region of the spinal cord. The ratio of the actual/expected dorsal column volume was used to assess the degree of expansion or contraction of the dorsal column as a result of X-EB lesioning or cell transplantation and to adjust gross lesion size to compensate for these changes (see formulas below). Maximum dorsal column cross-sectional areas in each experiment were also compared with the average maximal cross-sectional areas of two intact control dorsal columns.

The extent of myelin restoration in each experiment was estimated by dividing the total remyelinated axon length by the amount of myelinated axon length expected to be present in a comparably sized intact region of the dorsal column (see formulas below).

Selected formulas

$$k=\frac{\sum_{j=1}^{n-1} d\cdot\left[\frac{(A_{\mathrm{DC},j}+A_{\mathrm{DC},j+1})}{2}\right]}{1.0977\cdot n\cdot d\cdot\left[\frac{(A_{\mathrm{DC},j}+A_{\mathrm{DC},n})}{2}\right]}$$

$$V_{\mathrm{Les,Adj}}=\frac{1}{k}\cdot\sum_{j=1}^{n-1} d\cdot\left[\frac{(A_{\mathrm{Les},j}+A_{\mathrm{Les},j+i})}{2}\right]$$

$$M_{\mathrm{re,Total}}=\sum_{j=1}^{n-1}\mathrm{d}\cdot\left[\frac{\begin{array}{c}[(A_{\mathrm{R},j}\cdot D_{\mathrm{R},j})+(A_{\mathrm{P},j}\cdot \mathrm{D}_{\mathrm{P},j})]+\\ [(A_{\mathrm{R},j+1}\cdot D_{\mathrm{R},j+1})+(A_{\mathrm{P},j+1}\cdot D_{\mathrm{P},j+1})]\end{array}}{2}\right]$$

$$M_{\mathrm{restore}}=\frac{M_{\mathrm{re,Total}}}{V_{\mathrm{Les,Adj}}\cdot D_{\mathrm{c}}}$$

where: k = ratio of actual/expected dorsal column volumes d = distance between sections analyzed (usually 0.25 mm, unless sections were missing or damaged) j = rostral/caudal position along the dorsal column $A_{\mathrm{DC},j}$ j = cross-sectional area of dorsal column at position j $A_{\mathrm{Les,j}}$ = cross-sectional area of lesion at position j $A_{\mathrm{R},j}$ j = cross-sectional area of myelin-rich region at position j $A_{\mathrm{P},j}$ = cross-sectional area of myelin-poor region at position j $D_{\mathrm{R},j}$ = average remyelinated axon density in myelin-rich region at position j $D_{\mathrm{P},j}$ = average remyelinated axon density in myelin-poor region at position j D_{C} = average myelinated axon density in intact control dorsal column $V_{\mathrm{Les,Adj}}$ = lesion volume after adjusting for expansion or contraction of the dorsal column as a result of lesioning or cell transplantation $M_{\mathrm{re,Total}}$ = total remyelinated axon length (axon × mm) M_{restore} = % myelin restoration of ratio of total remyelinated axon length/myelinated axon length present in control region of the same size

Statistical analysis of data

Dorsal column sizes, total remyelination, percent remyelination, and maximal remyelinated axon densities in myelin-rich regions for each cell transplant condition were compared with control X-EB lesions using the unpaired Student's t-test and assuming unequal variance (Microsoft Excel 97 statistical tool pack). Effects of individual transplant parameters on remyelination were assessed using a MANCOVA (Systat for Windows) and controlling for lesion size and other donor cell characteristics. Correlation coefficients (corr.) between adjusted lesion volumes and total remyelination for each transplant protocols were calculated using the Microsoft Excel 97 statistical tool pack. Slopes and standard errors of best-fit lines were calculated using Origin 6 and assuming a Y intercept of zero. Two animals were eliminated from the study because total remyelination and percent myelin restoration differed from means for their respective protocols by more than 2 standard deviations and did not differ significantly from control lesions, implying a problem with the cell transplantation.

The basic protocol is summarized in Figure 1. See number values column in Table 1 for numbers of transplant recipients in each transplant condition. Transplants were performed in groups of 3 animals each with approximately 12 P3 pups, 4 P7 pups, or 1 adult rat used to isolate each batch of optic nerve astrocytes (ONAs) or neonatal or adult Schwann cells, respectively. Photomicrographs were constructed using Adobe Photoshop (San Jose, CA).

RESULTS

Morphology and sizes of lesions

Intact areas of the dorsal funiculus, as well as "myelin-rich" and "myelin-poor" regions within each lesion could be readily identified in plastic-embedded sections at low magnification by differences in staining density, corresponding to different densities of myelinated axons observed at higher magnification (Figs. 1–3). Discernment between remyelinated and intact regions of the spinal cord was further facilitated by a slight color shift from the blue-black of intact CNS myelin to a brighter blue in areas exhibiting Schwann cell-like patterns of myelination (color plates not included). Histological examination confirmed that the X-EB protocol consistently resulted in essentially complete demyelination of areas encompassing an average of 93 ± 2% of the targeted dorsal funicular area at the widest point (n = 81), with portions of the lateral aspects of the dorsal funiculus and/or the dorsal tip of the ventral horn also being affected in some experiments. Lateral boundaries of lesions were typically sharp and distinct across most of their length, but were somewhat irregular at rostral and caudal ends. Histologically identifiable lesions delineated slightly irregular elongated fusiform areas with an average gross volume of 1.19 ± 0.05 mm^3 (range 0.40 –2.65 mm^3) and an average length of 6.5 ± 0.2 mm (range 3.25–10.5 mm).

High-magnification (100×) images of control X-EB lesions without transplanted cells revealed that lesioned areas consisted primarily of densely packed nonmyelinated axons, phagocytic cells, and cell debris, with only an occasional intact myelinated axon observable within the lesion at any level of the cord (Fig. 2B′). In contrast, all lesions receiving transplanted rat Schwann cells contained large areas exhibiting many axonal profiles with the characteristic appearance of peripheral myelination (Berthold, 1978), i.e., individual axons surrounded by a dense band of membrane staining and prominent areas of cytoplasm. Within these myelin-rich areas, the majority of detectable axons were myelinated, although the spacing between axons was noticeably increased compared with either intact or myelin-poor regions, and scattered non-myelinated axons could also be identified within "myelin-rich" areas (Fig. 3). When all axons within regions classified in this study as myelin-rich were counted, an average of 52.4 ± 0.2% of detectable axons (including apparently degenerating axons and axons with intact myelin) exhibited peripheral-like patterns of myelination (n = 4,698 sampled regions in 31 Schwann cell transplanted lesions), and more than 30% of counted areas contained greater than 70% Schwann cell-like myelinated axon profiles.

Presumptive Schwann cell bodies were associated with the majority of resolvable axons within these "myelin-rich" areas, and the heavily stained bands surrounding these axons, as well as increased spacing, greatly facilitated counting of remyelinated axons. Nonmyelinated axons were much more difficult to resolve individually. We therefore did not use counts of nonmyelinated axons to assess the proportion of demyelinated axons that were remyelinated following cell transplantation, but instead relied on more indirect methods for determining the percentages of myelin restoration, as described below and in Materials and Methods.

In addition to the apparent remyelination observed in lesions receiving Schwann cell transplants, small numbers of Schwann cell-like myelinated axon profiles were also detected in lesions receiving transplanted ONAs (data not shown), but they were rarer than in any of the Schwann cell-transplanted conditions. In X-EB lesions with DMEM injections alone,

Schwann cell-like myelinated axon profiles were extremely rare or absent (Fig. 2B′) and were restricted almost exclusively to the dorsal surface of the column.

Effects of cell transplantation on dorsal column size

Comparisons between cross-sectional areas of intact control dorsal columns and X-EB lesioned dorsal columns with and without cell transplants revealed a small but noticeable contraction of dorsal columns with demyelinating lesions and an expansion of dorsal columns in some Schwann cell-transplanted animals. Maximal cross-sectional areas of X-EB-lesioned dorsal columns without cell transplantation, and total volumes of X-EB-lesioned dorsal columns were decreased by 25 ± 6% (n = 8) and 19 ± 6% (n = 8), respectively, compared with cross-sectional areas and volumes of dorsal column regions of comparable length (Fig. 4). Maximum cross-sectional areas and dorsal column volumes of the X-EB lesioned condition differ from intact controls at $P < 0.008$ and $P < 0.02$, respectively (unpaired Student's t-test).

Transplantation of Schwann cells, ONAs, or both into demyelinated lesions resulted in an increase in dorsal column volume and maximal cross-sectional area when compared with X-EB lesions without cell transplantation, but produced no statistically significant change in dorsal column size relative to the intact condition. Dorsal column volumes for spinal cords transplanted with ONAs only and for all Schwann cell-transplanted lesions averaged 101 ± 6% (n = 8) and 103 ± 3% (n = 70) of expected values, respectively, whereas maximal cross-sectional areas averaged 93 ± 7% (n = 8) and 95 ± 2% (n = 70), respectively, of intact dorsal columns (Fig. 4). Dorsal column volumes and maximal cross-sectional areas for all Schwann cell-transplanted conditions differed from X-EB lesions alone at $P < 0.006$ and $P < 0.002$, respectively. Dorsal column volumes for ONA transplants differed from X-EB lesions only at $P < 0.02$ (unpaired Student's t-test; see Table 1 for data summary).

Although none of the Schwann cell transplant protocols tested resulted in a statistically significant expansion of the dorsal column, relative to the intact condition, cross-sectional areas of dorsal columns receiving transplanted Schwann cells were much more variable along their lengths than those in either intact or X-EB lesion only condition (not shown), and they were also more variable between experiments. In a minority of experiments, Schwann cell transplantation did result in a considerable local expansion of dorsal column cross-sectional area and/or an increase in dorsal column volume. For example, in two Schwann cell-transplanted animals, maximal dorsal column cross-sectional areas exceeded average values for intact spinal cords by more than 50%, and in five animals, total dorsal column volume exceeded expected values by more than 30%. To compensate for any expansion or contraction of the regions studied, and obtain more accurate estimates of the amounts of axon length that were demeylinated, we therefore made the simplifying assumption of uniform expansion or contraction of the dorsal column and adjusted gross lesion volumes accordingly (see Materials and Methods).

Pattern of remyelination

In this study, Schwann cell-like myelination was never observed outside of the dorsal column region, except in a small number lesions that included portions of the ventral horn, which also exhibited peripheral-like myelinated axon profiles (not shown). This strict segregation of remyelinated axon profiles to regions normally containing white matter was observed even when lesions extended to the lateral edges of the dorsal column, eliminating any possible barrier to the free migration of Schwann cells into other regions of the spinal cord.

Although Schwann cell-like myelinated axon profiles were routinely found throughout the lengths of Schwann cell-transplanted lesions, and were present in all regions within the dorsal column, the distribution of Schwann cell-induced remyelination was noticeably nonuniform

in all transplant experiments. Two discrete types of regions could be readily detected in almost every section of Schwann cell-transplanted lesions examined; myelin-rich areas typically containing tens of thousands of Schwann cell-like myelinated axon profiles per mm^2 and very few nonmyelinated axons, and myelin-poor areas, containing only a few hundred or less remyelinated axons per mm^2 and numerous nonmyelinated axons. Large myelin-rich areas were detected in the centers of all Schwann cell-transplanted lesions examined (Fig. 3) and often extended rostrally and caudally along the entire length of the lesion (Fig. 5A). Myelin-rich areas, however, rarely filled the entire demyelinated region at any level of the lesion. Although myelin-poor areas encompassed a greater proportion of the lesion farther from the transplantation site, they could be found at all levels of lesions (Fig. 5A). It was also noted that in many cases, the shapes and positions of myelin-rich areas were very similar across many sections, suggesting a preferential spread of transplanted Schwann cells longitudinal to, rather than perpendicular to the axonal trajectory.

Densities of remyelinated axons in myelin-rich regions were fairly consistent along the length of any given lesion (Fig. 5B) and did not differ greatly between experiments, implying a preferential spacing pattern for transplanted Schwann cells. Although much lower than densities of myelinated fibers in intact dorsal columns, remyelinated axon densities in myelin-rich regions of X-EB lesions often approached those for myelinated fibers in intact sciatic nerve (Fig. 6). Myelin-rich regions of Schwann cell-transplanted dorsal columns contained an average of 32,000 ± 1,000 myelinated axons/mm^2 (n = 70) at the level of the lesion showing the highest density of remyelination, compared with 110,0000 ± 3,000 myelinated axons/mm^2 in the intact dorsal column and 43,000 myelinated axons/mm^2 in the intact sciatic nerve. These results indicated an increase in spacing between Schwann cell myelinated dorsal column axons compared with the intact cord. Maximum remyelinated axon densities were slightly higher for freshly isolated than cultured Schwann cells (33,000 ± 1,000 [n = 42] and 31,000 ± 2,000 [n = 28], respectively), but these differences were not statistically significant and donor ages, ONA co-transplantation, and immunosuppression also had no statistically significant effect on remyelinated axon density (Fig. 6).

Total transplant-induced remyelination

Quantitative analysis of Schwann cell remyelination under many different transplant protocols revealed that transplantation of 30,000 Schwann cells typically resulted in remyelination of tens of thousands of mm of total axon length (Fig. 7A). Total estimated remyelinated axon length for all Schwann cell-transplanted lesions in this study averaged 18,000 ± 1,000 axon × mm, compared with only 1,420 ± 600 and 5,000 ± 2,000 axon × mm in control lesions and ONA-only transplanted lesions, respectively. Remyelination of Schwann cell-transplanted lesions differed from control and ONA transplanted lesions at $P < 0.000001$ and $P < 0.0001$, respectively (unpaired Student's t-test). The vast majority of total remyelinated axon length, 87 ± 1% (n = 69), was localized to myelin-rich regions of lesions, but in some experiments, the generally larger myelin-poor areas contributed more than one-third of the total remyelinated length.

Although Schwann cells from donors of all ages and conditions significantly increased total remyelination, the extent of repair was greater under protocols using younger and freshly isolated cells than for protocols using Schwann cells from aged donors or previously cultured cells. Transplantation of neonatal, young adult, and aged adult Schwann cells resulted in remyelination of an average of 21,000 ± 2,000 (n = 26), 17,000 ± 1,000 (n = 37), and 12,000 ± 1,000 (n = 7) axon × mm of axonal length respectively. Total remyelination for neonatal, young adult, and aged adult donors differed from control lesions at $P < 0.000001$, $P < 0.000001$, and $P < 0.004$, respectively. Aged adult Schwann cells differed from neonatal cells and young adults at $P < 0.0002$ and $P < 0.006$, respectively (unpaired Student's *t*-test). Similarly,

transplantation of freshly isolated versus cultured Schwann cells resulted in remyelination of 20,000 ± 1,000 (n = 42) and 16,000 ± 2,000 (n = 28) axon × mm, respectively, although the increased remyelination using freshly isolated cells was only statistically significant when differences in lesion sizes were controlled.

ONA co-transplantation also slightly increased average total remyelination from 17,000 ± 1,000 (n = 45) to 19,000 ± 2,000 (n = 25) axon × mm. However, ONA co-transplantation appeared only to affect remyelination by cultured cells, increasing remyelination in cultured Schwann cell transplant protocols to approximately the levels observed in protocols using freshly isolated Schwann cells, but having no detectable influence on remyelination by freshly isolated Schwann cells. ONA-induced increases in Schwann cell remyelination were only statistically significant when both prior culture history and sizes of lesions were controlled. Host immunosuppression with cyclosporin (see Materials and Methods) had no statistically significant effect on total remyelination when compared either with identical protocols without immunosupression or with all other Schwann cell transplants. Total remyelination for freshly isolated young adult Schwann cells with immunosuppression, freshly isolated young adult Schwann cells without cyclosporin treatment, and all Schwann cell transplant protocols without immunosuppression averaged 23,000 ± 3,000 (n = 8), 18,000 ± 2,000 (n = 14), and 18,000 ± 1,000 (n = 62) axon × mm respectively.

Percent restoration of myelination

Although percentages of demyelinated axons remyelinated by transplanted Schwann cells could not be reliably measured in the study, due to difficulties in counting nonmyelinated axons (see Materials and Methods), comparisons between the total amounts of remyelinated axons length within Schwann cell-transplanted lesions and the amounts of myelinated axon length estimated to be present in comparable sized intact control dorsal column regions demonstrated that Schwann cell transplantation resulted in restoration of a substantial fraction of normal myelination levels within the 3-week period examined (Fig. 7B). Overall, transplantation of Schwann cells of all ages and cell histories resulted in restoration of an average of 14.2 ± 0.7% (n = 70) of the myelination levels in the intact condition. This compares with myelination rates of 1.6 ± 0.6% (n = 8) and 5 ± 1% (n = 3) for control lesions without cell transplantation and ONA only transplanted lesions, respectively. The small numbers of axons exhibiting peripheral-like patterns of myelination in control lesions could represent either low levels of Schwann cell myelination that may normally be present within dorsal columns or remyelination by endogenous Schwann cells migrating in from the peripheral nerve.

We emphasize that these myelin restoration values are expressed relative to the intact spinal cord. Because some axons may be lost as a result of the X-EB or transplant protocol, the percentage of available axons that were remyelinated may be higher. Schwann cell transplant protocols differed significantly from control lesions and the ONA-only transplantation protocol at $P < 0.000001$ and 0.001, respectively. ONA-only transplants differed from DMEM controls at $P < 0.06$. Average percentages of myelin restoration for individual transplant protocols ranged from 6% (n = 2) for cultured adult Schwann cells to 22 ± 3% (n = 3) for freshly isolated neonatal Schwann cells, with all protocols represented by more than two experiments being significantly increased over controls at $P < 0.03$ or better (unpaired Student's *t*-test).

Overall, higher percentages of repair were observed using freshly isolated Schwann cells from younger donors, compared with cultured cells or cells from older animals, and ONA co-transplantation increased the percent restoration of myelination in protocols using cultured Schwann cells. Differences in myelin restoration rates between transplant protocols were not statistically significant, however, unless other factors, such as lesion size, were controlled.

Effects of individual transplant parameters on the amount remyelination

To assess which aspects of Schwann cell transplantation protocols were most important for promoting successful remyelination, many different transplant protocols were compared. Schwann cells from neonatal, normal young adult, nerve-crushed young adult, or aged adult donors were transplanted into X-EB lesions, either immediately after cell isolation, or after several weeks in culture, with or without co-transplanted ONAs. In addition, eight animals transplanted with freshly isolated Schwann cells from young adult donors were given daily injections of cyclosporin in order to evaluate whether immunosuppression influenced remyelination. Possible influences of lesion size on subsequent repair were also assessed by comparing the total amounts of remyelination observed in lesions of different sizes that were subjected to the same transplant protocol.

Total remyelination for all Schwann cell-transplanted lesions correlated moderately with the adjusted lesion volumes (corr. 0.347725) and more weakly with lesion length and cross-sectional area (corr. 0.12816 and 0.20399, respectively), implying that the amount of target tissue available for remyelination affected the proliferation, migration, or rate of myelin formation of transplanted Schwann cells. Correlations between lesion size and total remyelination were much stronger for Schwann cells/ONA co-transplantation protocols than for Schwann cell-only transplants (corr. 0.612947, n = 25 and 0.158001, n = 45, respectively) and were slightly stronger for neonatal than adult donors (corr. 0.404384, n = 28 and 0.28153, n = 37, respectively). The strongest correlation between lesion size and total remyelination was found for the three ONA-only transplantation experiments (corr. 0.851882), whereas the weakest correlation was found in the eight control lesions without cell transplantation (corr. 0.012385).

The relationship among lesion sizes, individual Schwann cell transplantation parameters, and successful remyelination could best be appreciated when the total remyelination for many individual experiments was plotted as a function of lesion size (Fig. 8). After adjusting for any expansion or contraction of the targeted area as the result of the X-EB lesion or cell transplantation, all transplant conditions showed a tendency toward increased total remyelination with increasing lesion size (Fig. 8) However, when the slopes of the best-fit lines for data points representing different transplant protocols were compared, prior cell culturing (Fig. 8B,E), donor age (Fig. 8C,E), ONA co-transplantation (Fig. 8C,E), and prior crush of adult nerves (Fig. 8D,E) could each be seen to affect total remyelination.

When lesion size was controlled, Schwann cells from neonatal donors resulted in remyelination of more total axon length than cells from young adults, and cells from young adults remyelinated more axon length than cells from aged adults. Freshly isolated Schwann cells remyelinated more axon length than cultured cells, and cells from a previously crushed sciatic nerve remyelinated more axonal length than cells from normal undamaged nerves. All differences were significant at $P < 0.001$ or better (MAN-COVA). The effects of ONA co-transplantation were more complex. ONAs appeared to increase remyelination when co-transplanted with cultured Schwann cells ($P < 0.001$, MANCOVA) but had no effect when co-transplanted with freshly isolated Schwann cells of any age. Cyclosporin injections also slightly increased total remyelination, but the effects were not statistically significant, even when lesion size and all other transplant parameters were controlled.

DISCUSSION

In this study we investigated the remyelination potential of Schwann cells transplanted into demyelinated and agliotic spinal cord lesions. The results show that transplantation of a relatively small number of autologous Schwann cells can result in remyelination of a relatively large amount of CNS axon length, restoring a substantial fraction of normal myelination levels

within 3 weeks after transplantation. The data further demonstrate that although the total amount of remyelination can be influenced by transplant parameters such as donor age and prior cell history, Schwann cells of all ages, and under all transplant protocols tested, remyelinate spinal cord axons with similar patterns and densities. These observations imply that important aspects of the remyelination process are controlled by features inherent to the donor cell type, rather than donor age or the specific cell isolation and transplantation protocol.

Pattern of Schwann cell remyelination

The distribution of myelinated axon profiles within Schwann cell-transplanted X-EB lesions in this study was consistent with descriptions of Schwann cell dispersion from transplantation sites in focal injury models of spinal cord tracts (Li and Raisman, 1997; Imiazumi et al., 2000), thalamus (Brook et al., 1993), and hippocampus or fimbria (Raisman et al., 1993), as well as our previous studies of Schwann cells transplanted into X-EB lesions (Honmou et al., 1996). Taken together, the similarities in shapes of myelin-rich regions across several millimeters of the spinal cord, and the long rostral-caudal extent of these myelin-rich regions, which nonetheless rarely extended to the lateral margins of the lesion, strongly imply a preferential movement of Schwann cells parallel to axonal tracts. These observations suggest that transplanting Schwann cells at multiple sites perpendicular to the axonal trajectory would probably be more effective in remyelinating large lesions, than transplanting equal numbers of cells along the tract.

Assessment of myelin restoration potential

In this study, transplantation of 30,000 Schwann cells consistently resulted in remyelination of tens of thousands of millimeters of dorsal column axon length, regardless of donor age or prior cell history, and remyelinated more that 40,000 axon × mm in 10% of experiments. These relatively high values for total remyelinated axon length imply that either individual transplanted Schwann cells remyelinate unusually long internodal intervals, compared with those reported for rat peripheral nerve (Bowe et al., 1994; Hildebrand et al., 1987), or that transplanted Schwann cells can proliferate within demyelinated lesions, as has been reported for endogenous Schwann cells (Harrison, 1987). The observations that total remyelination correlated moderately with lesion size and that myelin-rich regions routinely extended along the entire rostral/caudal axis of the lesion further argue that Schwann cell movement and myelination were limited by the size of the lesion rather than the repair capabilities of the transplanted cells. Data showing that remyelinated axon densities in myelin-rich regions approached, but did not exceed, myelinated axons densities in the intact nerve further argue that Schwann cells remyelinate dorsal column axons in a cell type-specific pattern.

One simple interpretation for all these observations would be that the rate of Schwann cell myelination is dependent in part on the frequency of Schwann contact with appropriate demyelinated axons. As Schwann cell remyelination within a given region approaches the normal peripheral nervous system spacing (i.e., becomes saturated), the rate of remyelination in this region may slow, and Schwann cells may then move into regions containing greater numbers of unmyelinated axons. If this hypothesis is correct, then the total remyelination values reported in this study might underestimate the extent of repair possible in larger lesions or after longer time intervals.

The percentages of myelin restoration calculated for Schwann cell transplants in this study were significantly lower than our earlier repair estimates (Honmou et al., 1996), and those of others (Shields et al., 1999, 2000), who reported essentially complete remyelination in the centers of CNS lesions. The lower estimates of remyelination efficiency in this study, however, probably reflect different approaches to assessing repair rather than significant differences in the behavior of transplanted cells. Although counting both remyelinated and nonmyelinated

axons revealed that more than 70% of detectable axons in the centers of lesions commonly exhibited peripheral-like patterns of myelination, total numbers of axons were also reduced in demyelinated lesions (with or without cell transplantation). This finding indicated that significant numbers of axons were either lost or displaced as a result of X-EB lesioning or cell transplantation. Given the extreme difficulty in accurately counting nonmyelinated axons to assess axonal loss, we chose to compare myelin content in the transplanted condition with that in the intact dorsal column. This approach allowed us to assess more effectively differences in repair efficiencies between different transplant protocols and to compare transplanted lesions with the intact condition, but it may underestimate the remyelinating potential of Schwann cells transplanted into lesions with no significant axonal loss.

In this study, Schwann cells were always observed to myelinate axons at much lower densities than those found in intact dorsal columns. The increased distances between Schwann cell-myelinated axon profiles and myelinated axon profiles in the intact dorsal column appeared to be largely due to the large areas occupied by the nuclear and cytoplasmic regions of the Schwann cells. It is noteworthy that the maximum myelinated axons densities in myelin-rich regions of lesions were similar to myelinated axon densities in the intact sciatic nerve, implying that Schwann cell myelination of CNS axons repeats the peripheral pattern of myelination.

It has been suggested that oligodendrocytes, which make multiple myelin segments, may have evolved to economize space in the CNS (Olson, 1997). Schwann cell remyelination in the CNS may therefore not be able to support the same density of myelinated axons as oligodendrocytes. If this idea is correct, then myelination density in the peripheral nerve may represent a theoretical upper limit to the number of CNS axons that can be remyelinated by Schwann cell transplantation. However, remyelination of even a modest number of axons could be functionally beneficial. For example, sparing of as little as 5–10% of myelinated axons has been shown to lead to recovery of effective locomotion in a contusive spinal cord injury model in the cat (Blight, 1983; Blight and Decrescito, 1986). Data presented in this study suggest that transplantation of Schwann cells into a lesion that can support Schwann cell migration and myelination has the potential to restore normal myelin levels at a range of 14–39%.

Relative effectiveness of different Schwann cell transplant protocols

In this study, both donor cell history and donor age influenced the ability of transplanted Schwann cells to remyelinate chemically demyelinated dorsal column axons, with freshly isolated cells and cells from younger donors remyelinating greater total axonal lengths than cultured Schwann cells or cell from older donors. Contrary to our initial expectations, however, age of the donor appeared to have a slightly smaller effect on remyelination than prior cell culturing. For example, although freshly isolated neonatal Schwann cells remyelinated greater total axonal lengths than freshly isolated young adult Schwann cells, freshly isolated adult Schwann cells actually remyelinated slightly greater total axonal lengths than cultured neonatal Schwann cells, when lesion sizes were controlled.

The observations that Schwann cells of all ages and prior histories myelinated axons at considerable distances (several mm) from the transplant site, exhibited similar remyelination densities, and remyelinated similar total axonal lengths strongly imply that Schwann cells have a cell type-specific response to demyelinated CNS axons that can be only slightly altered by prior cell history or other manipulations. It is possible, therefore, that differences in the amount of repair under different transplant protocols may simply reflect different rates of repair for cells at different starting conditions, rather than fundamental differences in donor cell properties. If this tentative conclusion is supported by future studies, it suggests that age or history of donor cells may not be critical factors in determining transplant success.

The one possible exception to the apparent virtual interchangeability of different Schwann cell transplant protocols may be the reduction in both total remyelination and myelinated axon density observed in transplant protocols using cultured Schwann cells compared with freshly isolated cells. In agreement with others (Duncan et al., 1981; Blakemore and Crang, 1985), and previous work in our laboratory (Honmou et al., 1996), we found in initial tests that Schwann cells cultured under conditions designed to produce very pure Schwann cell cultures failed to migrate far from the transplantation site or to remyelinate significant numbers of axons. Only when they were co-transplanted with ONAs did these purified Schwann cells migrate more than a short distance from the transplantation site. Based on the differences in remyelination efficiencies we observed for different transplantation protocols, we suspect that some aspect(s) of the Schwann cell enrichment protocol may eliminate a subset of cells with a greater tendency to proliferate, migrate, and myelinate axons. Our cell culture protocols may therefore inadvertently select for cells that are less able to remyelinate CNS axons. Alternatively, elimination of fibroblasts might have a detrimental effect on Schwann cell remyelination, because fibroblasts can facilitate Schwann cell ensheathment of axons (Obremski et al., 1993). It is also possible that axon membrane fragments present in freshly isolated Schwann cell preparations may stimulate Schwann cell proliferation in vivo, as has been shown in vitro (Wood and Bunge, 1975; Bigbee et al., 1987).

CONCLUSIONS

The present study demonstrates that Schwann cells from a wide range of donor ages, and prepared under many different cell isolation protocols, can lead to relatively extensive remyelination of CNS axons when transplanted into demyelinated spinal cord lesions. The amount of remyelination was, however, moderately greater in protocols using freshly isolated Schwann cells than cultured cells, and for cells derived from younger donors. Cyclosporin treatment did not inhibit remyelination. One must be cautious in attempting to extrapolate these results using an agliotic X-EB lesion rat model to pathological conditions where astrocytes are present. The interactions between Schwann cells and demyelinated or damaged axons (Wood and Bunge, 1975; Bigbee et al., 1987; Li et al., 1999), astrocytes (Franklin et al., 1993; Ghirnkar and Eng, 1994; Guénard et al., 1994a,b), glial progenitor cells (Franklin et al., 1992; Blakemore et al., 1995; Franklin et al., 1993), and fibroblasts (Obremski et al., 1993) are highly complex. Astrocytes in particular appear to have properties that can either inhibit or facilitate Schwann cell migration, with the net result being influenced by the relative proportion of the two cell types (Franklin et al., 1993; Ghirnkar and Eng, 1994; Guénard et al., 1994a,b), as well as the presence or absence of O2A progenitor cells (Blakemore and Crang, 1989; Franklin et al., 1992; Blakemore and Franklin, 1995) and possibly the age of the host (Shields et al., 1999). It is therefore not possible to predict whether transplanted Schwann cells would produce comparable levels of repair in the astrocyte-rich environment of an MS lesion or contusive injury. However, it is encouraging that the myelin restoration estimates in this study were sufficiently high that they do not rule out the possibility of a therapeutic benefit from Schwann cell transplantation.

Acknowledgements

NIH; Grant number: NS10174; Grant sponsor: the National Multiple Sclerosis Society; Grant number: RG2135; Grant sponsor: the Medical and Rehabilitation Research and Development Services of the Department of Veterans Affairs; Grant sponsor: the American Paralysis Association; Grant number: LA2-902.

Supported in part by the National Institutes of Health (NS10174), the National Multiple Sclerosis Society, and the Rehabilitation and Medical Research Services of the Department of Veterans Affairs. K.L.L. was the recipient of grant LA2-902 from the American Paralysis Association. Some of this work has been presented in abstract form (Lankford et al., 1998.)

Abbreviations

Ad
adult

CNS
central nervous system

Cult
cultured

Fr
fresh

Neo
neonatal

ONA
optic nerve astrocyte

Sch
Schwann cell

X-EB
ethidium bromide-irradiated

LITERATURE CITED

Barnett SC, Alexander CL, Iwashita Y, Gilson JM, Crowther J, Clark L, Dunn LT, Papanastassiou V, Kennedy PG, Franklin RJ. Identification of a human olfactory ensheathing cell that can effect transplant-mediated remyelination of demyelinated CNS axons. Brain 2000;123:1581–1588. [PubMed: 10908188]

Baron-Van Evercooren A. Schwann call transplantation and myelin repair of the CNS. Multiple Sclerosis 1997;3:157–161. [PubMed: 9291173]

Baron-Van Evercooren A, Gansmuller A, Duhamel E, Pascal F, Gumpel M. Repair of a myelin lesion by Schwann cells transplanted into the adult mouse spinal cord. J Neuroimunol 1992;40:235–242.

Baron van Evercooren A, Duhameal-Clerin E, Bounty JM, Hauw JJ, Gumpel M. Pathways of migration of transplanted Schwann cells in the demyelinated mouse spinal cord. J Neurosci Res 1993;35:428–438. [PubMed: 7689657]

Berthold, CH. Morphology of normal peripheral axons. In: Waxman, SG., editor. Physiology and pathobiology of axons. New York: Raven Press; 1978. p. 3-64.

Bigbee JW, Yoshino JE, De Vries GH. Morphological and proliferative responses of cultured Schwann cells following phagocytosis of a myelin-enriched fraction. J Neurocytol 1987;16:487–496. [PubMed: 3681350]

Blakemore WF. Remyelination of CNS axons by Schwann cells transplanted from sciatic nerve. Nature 1977;266:68–69. [PubMed: 840300]

Blakemore WF, Crang AJ. The use of autologous Schwann cells to remyelinate areas of persistent demyelination in the central nervous system. J Neurol Sci 1985;70:207–223. [PubMed: 4056820]

Blakemore WF, Crang AJ. The relationship between type-1 astrocytes, Schwann cells and oligodendrocytes following transplantation of glial cell cultures into demyelinating lesions in the adult rat spinal cord. J Neurocytol 1989;18:519–528. [PubMed: 2809635]

Blakemore WF, Franklin RJ. Transplantation options for therapeutic central nervous system remyelination. Cell Transplant 2000;9:289–94. [PubMed: 10811401]

Blakemore WF, Patterson RC. Suppression of remyelination in the CNS by X-irradiation. Acta Neuropathol (Berl) 1978;42:105–113. [PubMed: 654883]

Blakemore WF, Crang AJ, Evans RJ, Patterson RC. Rat Schwann cell remyelination of demyelinated cat CNS axons: evidence that injection of cell suspensions of CNS tissue results in Schwann cell remyelination. Neurosci Lett 1987;77:15–19. [PubMed: 3601212]

Blakemore WF, Crang AJ, Franklin RJM, Tang K, Ryder S. Glial cell transplants that are subsequently rejected can be used to influence regeneration of glial cell environments in the CNS. Glia 1995;13:79–91. [PubMed: 7649617]

Blight AR. Cellular morphology of chronic spinal cord injury in the cat: analysis of myelinated axons by line-sampling. Neuroscience 1983;10:521–543. [PubMed: 6633870]

Blight AR, Decrescito V. Morphometric analysis of experimental spinal cord injury in the cat: the relation of injury intensity to survival of myelinated axons. Neuroscience 1986;19:321–341. [PubMed: 3785669]

Blight AR, Young W. Central axons in injured cat spinal cord recover electrophysiological function following remyelination by Schwann cells. J Neurol Sci 1989;91:15–34. [PubMed: 2746287]

Bowe CM, Johansson CS, Hildebrand C, Evans NH. Functional properties of nodal spacing of myelinated fibers in developing rat mental and sural nerves. Dev Brain Res 1994;79:186–194. [PubMed: 7955317]

Brockes JP, Fields KL, Raff MC. Studies on cultured rat Schwann cells. I. Establishment of purified populations from cultures of peripheral nerve. Brain Res 1979;165:105–108. [PubMed: 371755]

Brook GA, Lawrence JL, Raisman G. Morphology and migration of cultured Schwann cells transplanted into the fimbria and hippocampus in adult rats. Glia 1993;9:292–304. [PubMed: 8112822]

Brook GA, Lawrence JM, Shah B, Raisman G. Extrusion transplantation of Schwann cells into the adult rat thalamus induces directional host axon migration. Exp Neurol 1994;126:31–43. [PubMed: 8157125]

Duncan ID, Milward EA. Glial cell transplants: experimental therapies of myelin diseases. Brain Pathol 1995;5:301–310. [PubMed: 8520730]

Duncan ID, Aguayo AJ, Bunge RP, Wood PM. Transplantation of rat Schwann cells grown in tissue culture into the mouse spinal cord. J Neurol Sci 1981;49:241–252. [PubMed: 7217983]

Duncan ID, Hammang JP, Jackson KF, Wood PM, Bunge RP, Langford KL. Transplantation of oligodendrocytes and Schwann cells into the spinal cord of the myelin-deficient rat. J Neurocytol 1988;17:351–360. [PubMed: 3171610]

Feigin I, Ogata J. Schwann cells and peripheral myelin within human central nervous tissues: the mesenchymal character of Schwann cells. J Neuropathol Exp Neurol 1971;30:603–612. [PubMed: 5135015]

Feigin I, Popoff N. Regeneration of myelin in multiple sclerosis: the role of mesenchymal cells in such regeneration and in myelin formation in the peripheral nervous system. Neurology (Mineap) 1966;16:364–372.

Felts PA, Smith KJ. Conduction properties of central nerve fibers remyelinated by Schwann cells. Brain Res 1992;574:178–192. [PubMed: 1638392]

Franklin RJM, Blakemore WF. Requirements for Schwann cell migration within CNS environment: a viewpoint. Int J Dev Neurosci 1993;11:641–649. [PubMed: 8116476]

Franklin RJM, Crang AJ, Blakemore WF. Type-1 astrocytes fail to inhibit Schwann cell remyelination of CNS axons in the absence of cells from the O-2A lineage. Dev Neurosci 1992;14:85–92. [PubMed: 1396178]

Franklin RJM, Crang AJ, Blakemore WF. The reconstruction of an astrocytic environment in glial deficient areas of white matter. J Neurocytol 1993;22:382–396. [PubMed: 8315415]

Franklin RJ, Bayley SA, Milner R, French-Constant CF, Blakemore WF. Differentiation of the O-2A progenitor cell line CG-4 into oligodendrocytes and astrocytes following transplantation into glia deficient areas of CNS white matter. Glia 1995;1:39–44. [PubMed: 7751054]

Ghatak NR, Hirano A, Doron Y, Zimmerman HM. Remyelination in multiple sclerosis with peripheral type myelin. Arch Neurol 1973;29:262–267. [PubMed: 4728187]

Ghirnkar RS, Eng LF. Astrocyte-Schwann cell interaction in culture. Glia 1994;11:367–377. [PubMed: 7960039]

Griffiths IR, McCulloch MC. Nerve fibers in spinal cord impact injuries. Part 1. Changes in myelin sheath during the initial 5 weeks. J Neurol Sci 1983;58:335–349. [PubMed: 6842262]

Guénard V, Aebischer P, Bunge RP. The astrocyte inhibition of peripheral nerve regeneration is reversed by Schwann cells. Exp Neurol 1994a;126:44–60.

Guénard V, Aebischer P, Bunge RP. Astrocytes inhibit Schwann cell proliferation and myelination of dorsal root ganglion neurons in vitro. J Neurosci 1994b;14:2980–2992.

Gumpel M, Bauman N, Raul M, Jaque C. Survival and differentiation of oligodendrocytes from neural tissue transplanted into newborn mouse brain. Neurosci Lett 1983;37:307–311. [PubMed: 6193461]

Gumpel M, Lachapelle F, Gansmuller A, Baulac M, Baron-Van Evercooren A, Baumann N. Transplantation of human embryonic oligodendrocytes into shiverer brain. Ann NY Acad Sci 1987;495:71–85. [PubMed: 3300467]

Harrison BM. Schwann cells divide in a demyelinating lesion of the central nervous system. Brain Res 1987;409:163–168. [PubMed: 3580865]

Harrison BM, McDonald WI. Remyelination after transient experimental compression of the spinal cord. Ann Neurol 1977;1:542–551. [PubMed: 883766]

Hildebrand C, Mustafa CY, Bowe C, Kocsis JD. Nodal spacing along regenerating axons following a crush lesion of the developing rat sciatic nerve. Brain Res 1987;429:147–154. [PubMed: 3567658]

Honmou O, Felts PA, Waxman SG, Kocsis JD. Restoration of normal conduction properties in demyelinated spinal cord axons in the adult rat by transplantation of exogenous Schwann cells. J Neurosci 1996;16:3199–3208. [PubMed: 8627358]

Hughes JT, Brownel B. Aberrant nerve fibers within the spinal cord. J Neurol Neurosurg Pychiatry 1963;26:528–534.

Imaizumi T, Lankford KL, Waxman SG, Greer CA, Kocsis JD. Transplanted olfactory ensheathing cells remyelinate and enhance axonal conduction in the demyelinated dorsal columns of adult rats. J Neurosci 1998;18:6176–6185. [PubMed: 9698311]

Imaizumi T, Lankford KL, Burton WV, Fodor WL, Kocsis JD. Xeno-transplantion of pig olfactory ensheathing cells promotes axonal regeneration in the rat spinal cord. Nat Biotechnol 2000;18:949–953. [PubMed: 10973214]

Itoyama Y, deF Webster H, Richardson EP Jr, Tramp BD. Schwann cell remyelination of demyelinated axons in spinal cord multiple sclerosis. Ann Neurol 1983;14:339–346. [PubMed: 6195956]

Itoyama Y, Ohnishi A, Tateichi J, Kuroiwa Y, deF Webster H. Spinal cord multiple sclerosis lesions in Japanese patients: Schwann cell remyelination occurs in areas that lack glial fibrallary acidic protein (GFAP). Acta Neuropathol 1985;65:217–223. [PubMed: 2579518]

Iwashita Y, Fawcett JW, Crang AJ, Franklin RJM, Blakemore WF. Schwann cells transplanted into normal and X-irradiated adult white matter do not migrate extensively and show poor long-term survival. Exp Neurol 2000;164:292–302. [PubMed: 10915568]

Kato T, Honmou O, Uede T, Hashi K, Kocsis JD. Transplantation of human olfactory ensheathing cells elicits remyelination of demyelinated rat spinal cord. Glia 2000;30:209–218. [PubMed: 10756071]

Lankford KL, Imiazumi T, Kocsis JD. Effects of donor age, prior cell history, and immunosuppression on remyelination of rat spinal cord axons by transplanted Schwann cells. Soc Neurosci Abstr 28 1998:793.4.

Li Y, Raisman G. Integration of transplanted cultured Schwann cells into the long myelinated fiber tracts of the adult spinal cord. Exp Neurol 1997;145:397–411. [PubMed: 9217076]

Li Y, Fields PM, Raisman G. Death of oligodendrocytes and micorgolia phagocytosis of myelin precede immigration of Schwann cells into the spinal cord. J Neurocytol 1999;28:417–427. [PubMed: 10739580]

McCarthy KD, de Vellis J. Preparation of separate astroglia and oligodendroglia cell cultures from rat cerebral tissue. J Cell Biol 1980;85:890–902. [PubMed: 6248568]

Mirsky R, Winter J, Abney EA, Pruss RM, Gavrilovic J, Raff M. Myelin-specific proteins and glycolipids in rat Schwann cells and oligodendrocytes in culture. J Cell Biol 1980;84:483–494. [PubMed: 7358790]

Obremski VJ, Johnson MI, Bunge MB. Fibroblasts are required for Schwann cell basal lamina deposition and ensheathment of unmyelinated sympathetic neurites in culture. J Neurocytol 1993;22:102–117. [PubMed: 8445407]

Ogata J, Feigin I. Schwann cells and regenerated peripheral myelin in multiple sclerosis: an ultrastructural study. Neurology (Minneap) 1975;25:713–716. [PubMed: 1171404]

Olson L. Regeneration in the adult central nervous system: experimental repair strategies. Nat Med 1997;3:1329–1335. [PubMed: 9396602]

Perry VH, Hayes L. Lesion-induced myelin formation in the retina. J Neurocytol 1985;14:297–307. [PubMed: 2413175]

Prineas JW, Connell F. Remyelination in multiple sclerosis. Ann Neurol 1979;5:22–31. [PubMed: 426466]

Prineas JW, Barnard RO, Kwon EE, Shaer LR, Cho ES. Multiple sclerosis: remyelination of nascent lesions. Ann Neurol 1993;1:33, 137–151.

Raisman G, Lawrence JM, Brook GA. Schwann cells transplanted into the CNS. Int J Dev Neurosci 1993;11:651–669. [PubMed: 8116477]

Rodriguez M. Central nervous system demyelination and remyelination in multiple sclerosis and viral disease models. J Neuro Immunol 1992;40:255–264.

Shields SA, Gilson JM, Blakemore WF, Franklin RJM. Remyelination occurrs as extensively but more slowly in old rats compared to young rats following gliotoxin-induced CNS demyelination. Glia 1999;28:77–83. [PubMed: 10498825]

Shields SA, Blakemore WF, Franklin RJM. Schwann cell remyelination is restricted to astrocyte-deficient areas after transplantation into demyelinated adult rat brain. J Neurosci Res 2000;60:571–578. [PubMed: 10820427]

Trotter J, Crang AJ, Schachner M, Blakemore WF. Lines of glial precursor cells immortalized with a temperature-sensitive oncogene give rise to astrocytes and oligodendrocytes following transplantation into demyelinated lesion in the central nervous system. Glia 1993;9:25–40. [PubMed: 8244529]

Wood PM, Bunge RP. Evidence that sensory axons are mitogenic for Schwann cells. Nature 1975;256:662–664. [PubMed: 1171378]

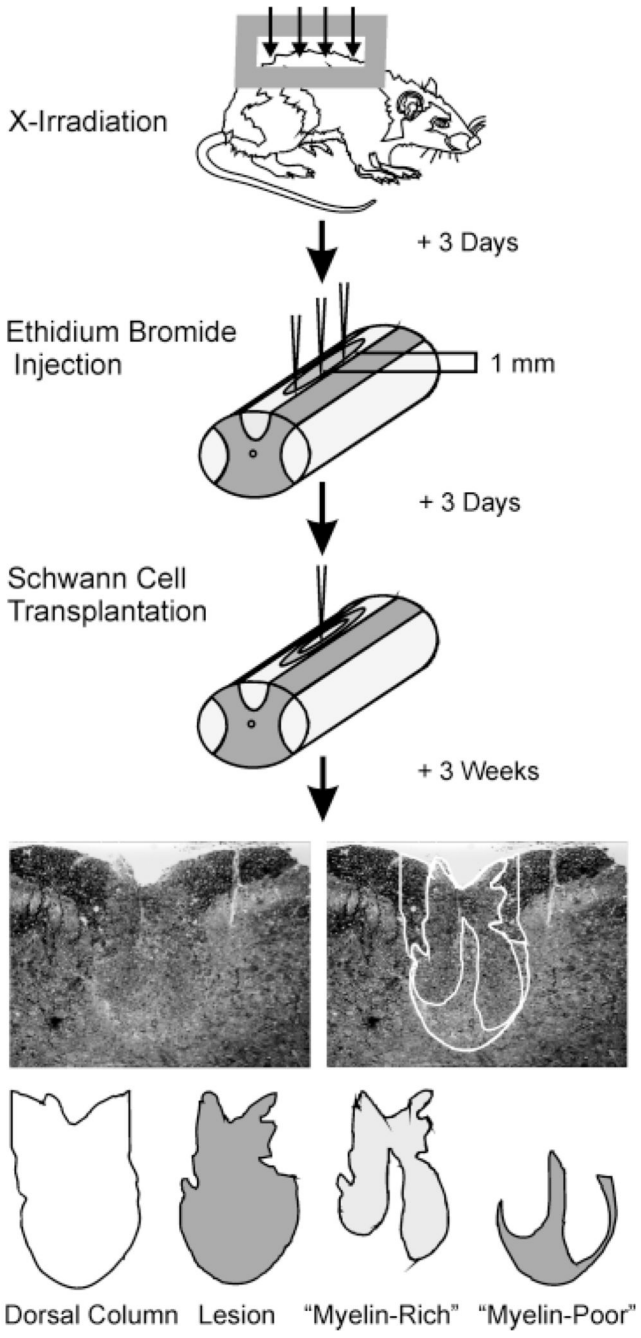

Fig. 1.

Diagram illustrating the basic protocol used in this study. Demyelinating lesions were created in the dorsal columns of adult rats using X-irradiation and ethidium bromide injections. Cells were transplanted into the centers of lesions, and rats were sacrificed 3 weeks after transplantation. Spinal cords were processed for histological analysis, and cross-sectional areas of the dorsal funiculus, the lesion, and "myelin-rich" and "myelin-poor" areas within the lesion were measured and densities of myelinated axons were counted within each region at 0.25-mm intervals along the spinal cord. These values were used to calculate the total amount of axon length remyelinated and to estimate the percentage of myelin restoration.

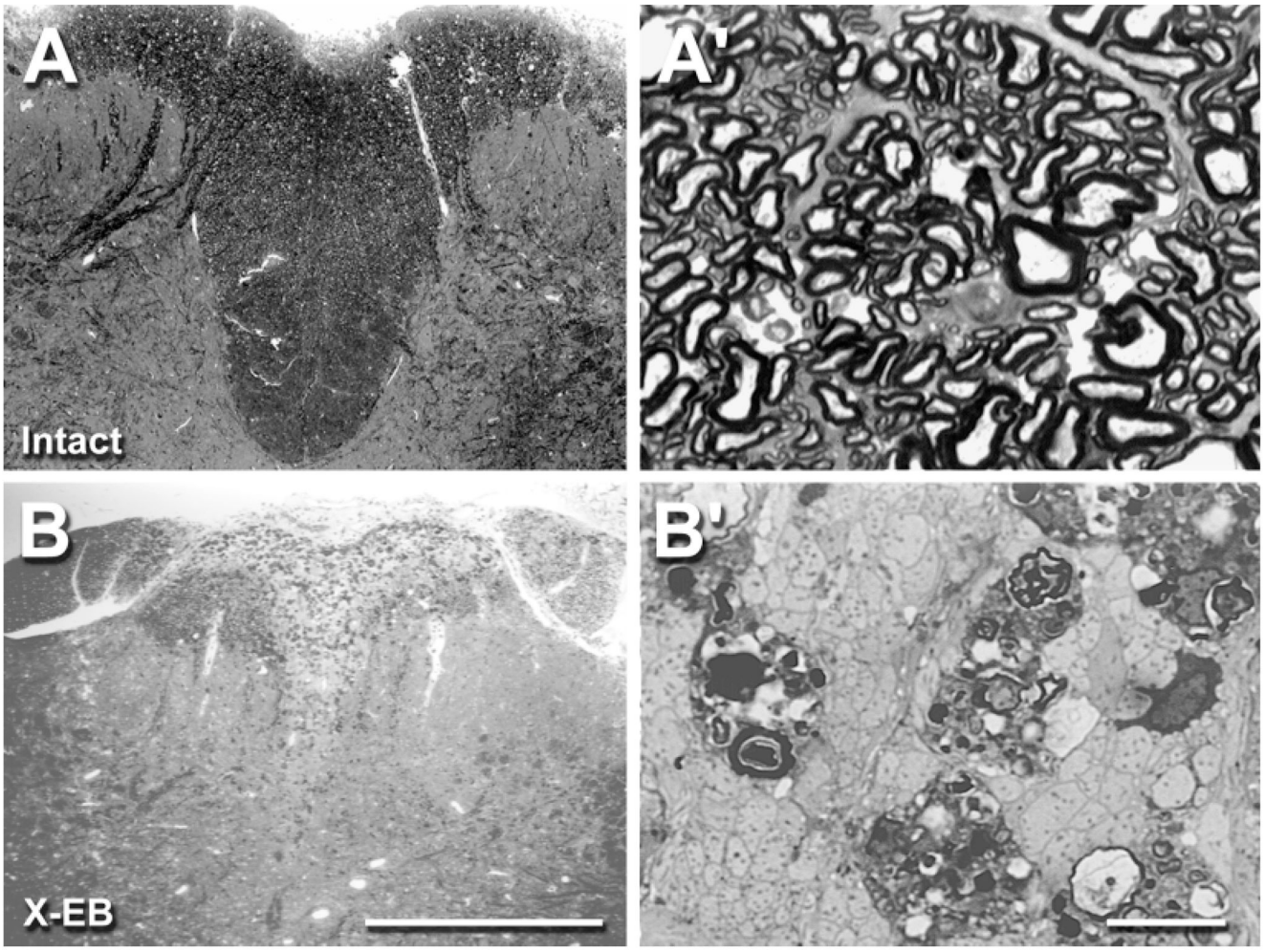

Fig. 2.

Photomicrographs illustrating cross sections of a representative intact (**A**, **A′**) and X-EB-lesioned adult rat dorsal column (**B**, **B′**). Pairs of micrographs show low (A, B) and high (A′, B′) magnification images taken in the center of an X-EB lesion and at the same spinal cord level in an intact control animal. High densities of myelinated fibers and relatively few nonmyelinated fibers were observed in the intact control dorsal column, whereas X-EB lesioned areas consisted almost exclusively of nonmyelinated axon profiles, phagocytotic cells, and myelin debris. Note the slight reduction in dorsal column area in the X-EB-lesioned condition compared with the intact dorsal column, which was typical of X-EB lesions without cell transplantation. All photomicrographs were digitally captured with an Image 1 processing system, with signal averaging and contrast enhancement. For abbreviations, see list. Scale bars = 0.5 mm in B; 0.01 mm in B′.

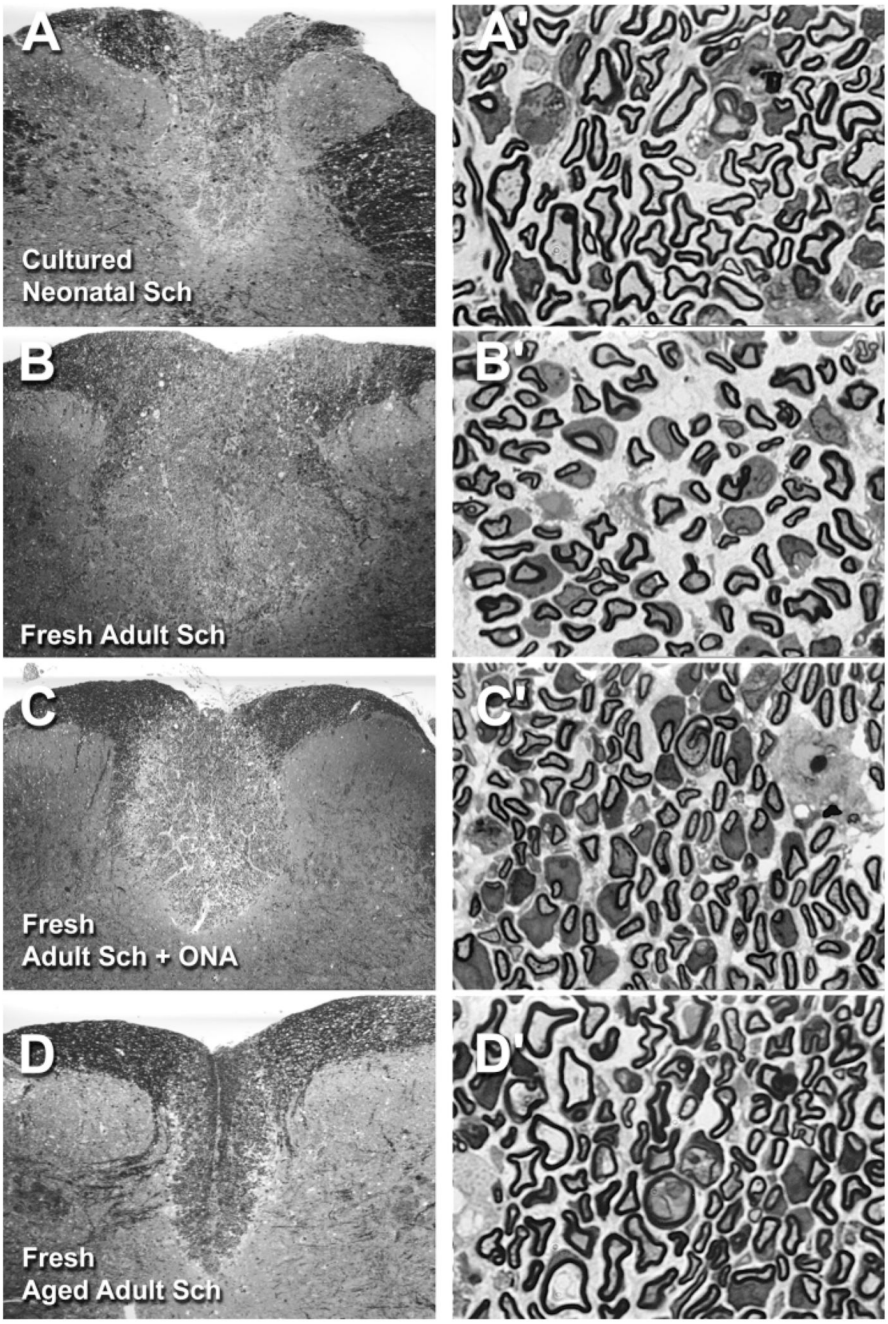

Fig. 3.

Photomicrographs of representative X-EB lesions with transplanted Schwann cells. Low and high magnification pairs of photomicrographs were taken in the centers of demyelinated lesions transplanted with 30,000 cultured neonatal Schwann cells (**A**, **A′**), freshly isolated young adult Schwann cells (**B**, **B′**), freshly isolated young adult Schwann cells with 20,000 cultured optic nerve astrocytes (ONAs) (**C**, **C′**), and freshly isolated aged adult Schwann cells (**D**, **D′**). Note the characteristic peripheral-like pattern of myelination and increased spacing between myelinated axons in each of the high magnification images, which was evident in all Schwann cell-transplanted conditions compared with the intact condition (Fig. 2A′), and the apparent slight expansion of dorsal column area in A–C, which was common to many Schwann cell-

transplanted lesions. Overall appearances of all other Schwann cell-transplanted conditions were similar to those shown here. For abbreviations, see list. See Figure 2 for scale bars: left panels = 0.5 mm, and right panels = 0.01 mm.

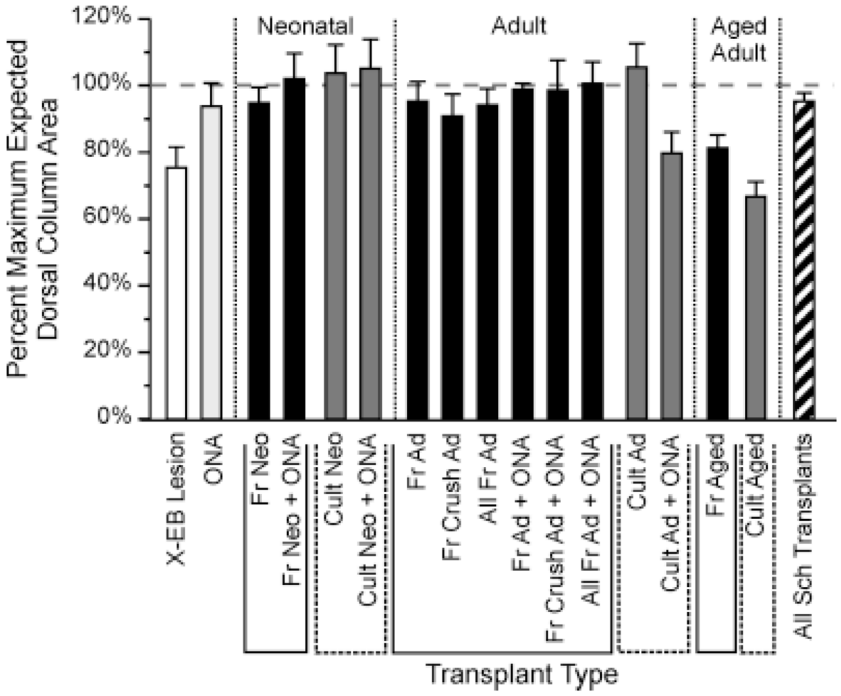

Fig. 4.

Bar graph illustrating the effects of X-EB lesions and Schwann cell transplantation on local dorsal column expansion or contraction. Each bar represents the average value for the ratio of the maximum cross-sectional of the dorsal column in the experimental condition compared with that of the intact control dorsal column. White and light gray bars represent control lesions without cell transplantation and control ONA transplants. Solid black and dark gray bars represent transplant protocols using freshly isolated and cultured cells, respectively. Diagonally striped bar represents all Schwann cell transplantation experiments in this study. Vertical dotted lines above the ordinate demarcate groups of protocols using Schwann cells from neonatal (Neo), adult (Ad), or aged adult (Aged) donors, respectively. Solid and dashed lines below the X-axis bracket groups of transplant protocols using freshly isolated (Fr) and cultured (Cult) cells, respectively. N values from left to right were 8, 3, 3, 5,10, 8, 17, 5, 22, 2, 5, 7, 2, 6, 5, 2, and 70, respectively. Labeling conventions and N values also apply to Figures 6 and 7 (see also Table 1). Note that although dorsal column sizes were increased under cell transplantation protocols when compared with X-EB lesions alone, significant expansions of dorsal columns beyond sizes found in intact control animals were rare. Maximal cross-sectional areas for all Schwann cell-transplanted conditions differed significantly from X-EB lesions alone at $P < 0.006$. Cross-sectional areas of dorsal columns receiving transplants of freshly isolated neonatal Schwann cells alone, freshly isolated neonatal Schwann cells + ONAs, cultured neonatal Schwann cells, freshly isolated adult Schwann cells alone, and freshly isolated adult Schwann cells + ONAs each differed from X-EB lesions alone at $P < 0.02$ or better (unpaired Student's t-test). For other abbreviations, see list.

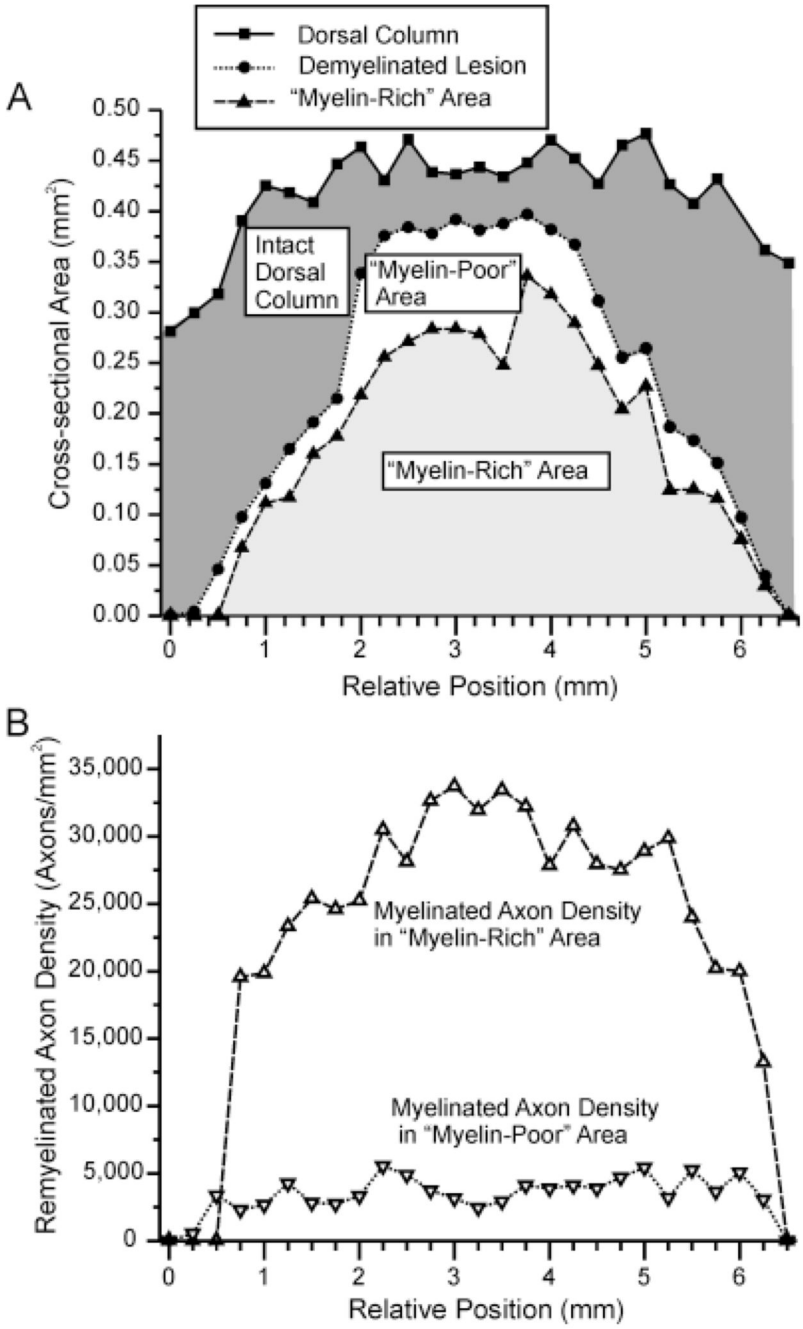

Fig. 5.

Line graphs illustrating the relative distributions and densities of remyelinated axons along the longitudinal axis of a representative X-EB lesion transplanted with 30,000 freshly isolated Schwann cells from a normal young adult rat sciatic nerve. **A:** Line graph showing cross-sectional areas of the targeted dorsal column area, demyelinated lesion, and myelin-rich region within the lesion at successive 0.25-mm intervals along the rostral/caudal axis. Filled squares, filled circles, and filled triangles, respectively, represent the cross-sectional areas of the entire dorsal column, demyelinated lesion, and myelin-rich region within the lesion. Shaded areas under curves indicate the volumes of the intact or undemyelinated area of the dorsal column, and the myelin-rich and myelin-poor regions within the lesion. Note that the myelin-rich region

extends almost throughout the length of the lesion but does not fill the lesion completely at any level. **B:** Line graph showing the densities of remyelinated axons in myelin-rich and myelin-poor areas along the rostral/caudal axis for the same lesion shown in A. Note the sharp differences between myelinated axon densities in the myelin-rich and poor areas and the relatively uniform density of myelinated axons throughout most of the lesion.

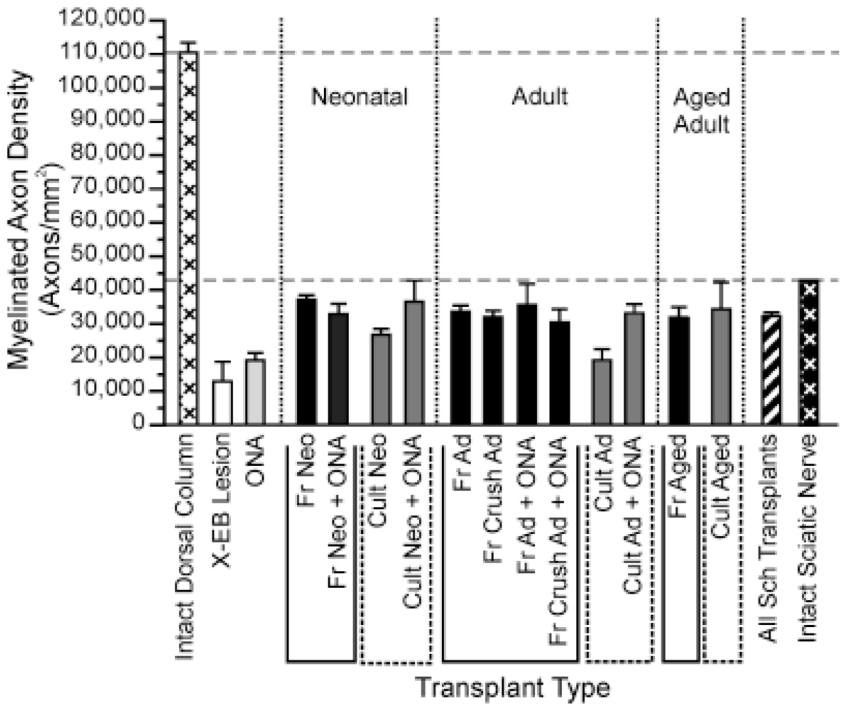

Fig. 6.

Bar graph comparing the highest densities of remyelinated axons observed in myelin-rich areas of Schwann cell-transplanted lesions with myelinated axon densities in intact rat dorsal column and sciatic nerve. Maximum myelinated axon density was defined as the average myelinated axon density in the myelin-rich area of the lesion at the level of the cord with the highest myelinated axon density. Note that maximal myelinated axon densities in Schwann cell-transplanted lesions approached values for intact sciatic nerve (black bars with white cross-hatching) but were much lower than myelinated axon densities in intact dorsal columns (white bars with black cross-hatching). See Figure 4 or Table 1 for N values. For abbreviations, see list.

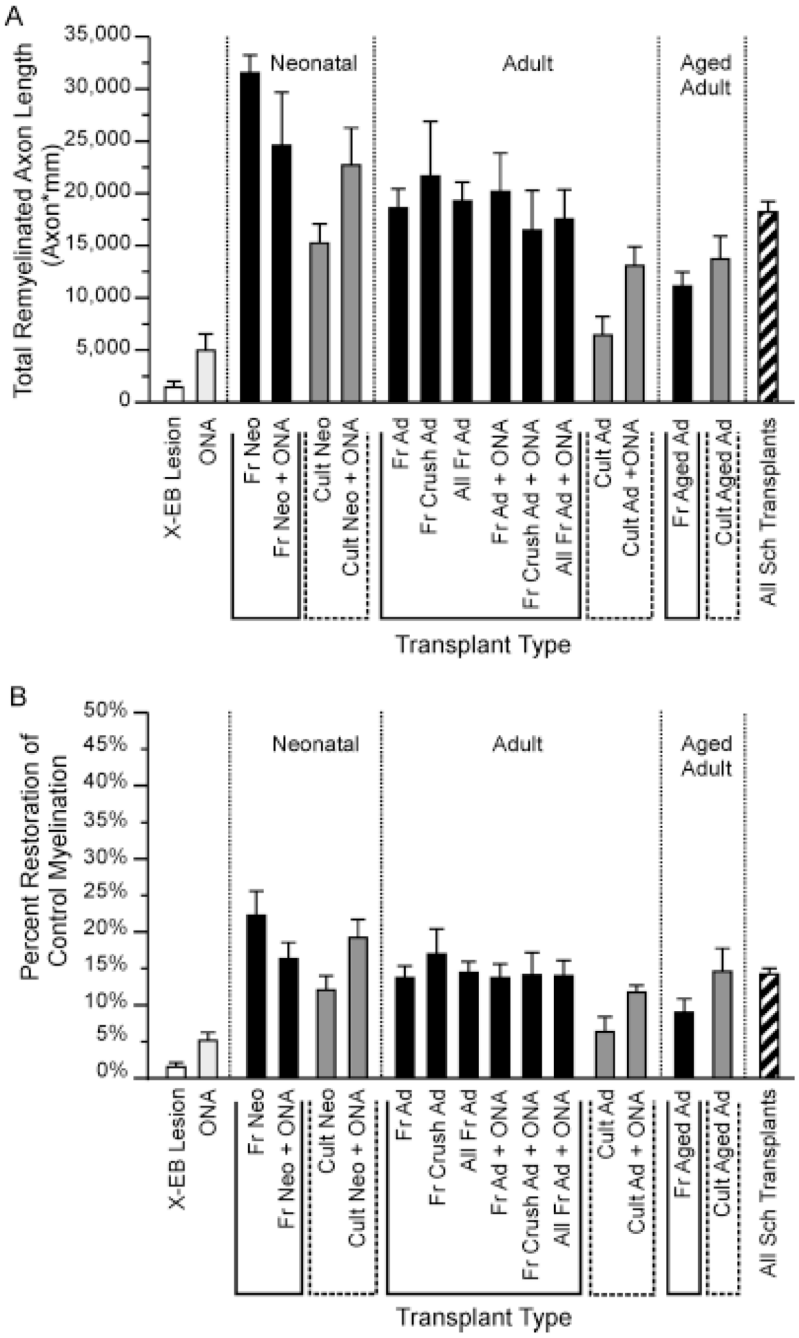

Fig. 7.

Bar graphs summarizing total remyelination (**A**) and percent restoration of intact myelination levels (**B**) observed under many different transplant protocols. (See Materials and Methods for formulas.) Note that transplantation of Schwann cell from donors of any age, with or without ONA co-transplantation, resulted in an increase in both total remyelination and percentage of myelin restoration. Both total remyelination ($M_{re,Total}$) and percent myelin restoration ($M_{restore}$) for all Schwann cell-transplanted lesions differ significantly from DMEM-only controls and ONA-transplanted lesions at $P < 0.000001$ and $P < 0.001$, respectively (unpaired Student's *t*-test). Percent myelin restoration in ONA-only transplant lesions was also increased over DMEM controls at $P < 0.06$, and total remyelination and percent myelin restoration for

each individual cell transplantation protocol, represented by more than two experiments, were increased over controls at $P < 0.03$ or better (unpaired Student's *t*-test). See Figure 4 for or Table 1 for N values. For abbreviations, see list.

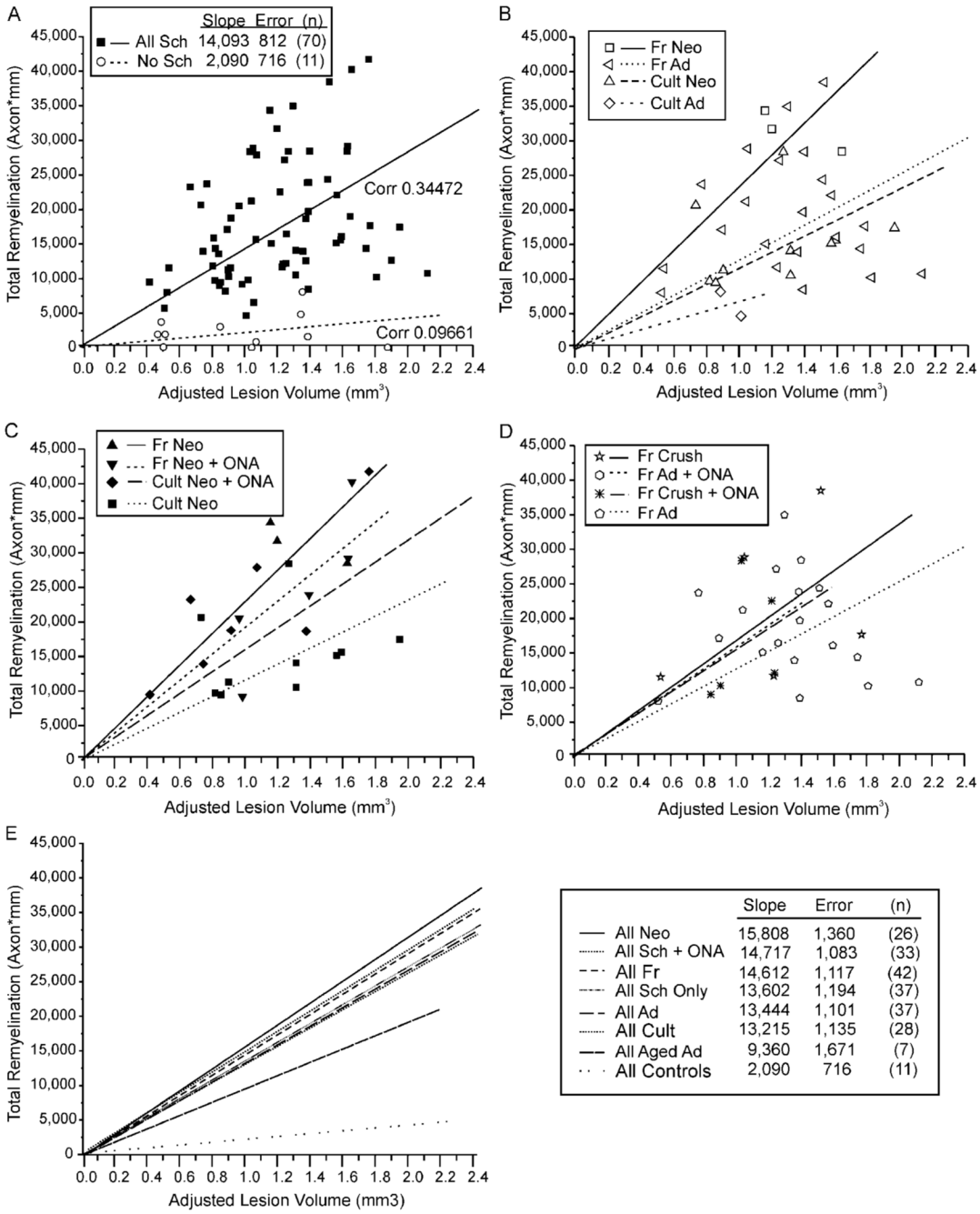

Fig. 8.

Relationships among lesion size, individual transplant parameters, and total remyelination for all transplantation protocols (A) and for selected subsets of experiments (B–D). One data point has been suppressed to enhance data separation. **A:** Summary of remyelination for all protocols. Total remyelination ($M_{re,Totall}$) for each experiment is plotted as a function of adjusted lesion size ($V_{Les,Adj}$). Best-fit lines and correlation coefficients (Corr) are shown for data points representing all control lesions with either DMEM or ONA-only injections, and all Schwann cell-transplant protocols. Note that total remyelination tends to increase with increasing lesion size. **B:** Relative influences of donor cell age and prior culturing on Schwann cell remyelination. Graph plots individual data points and best-fit lines for transplant protocols

using freshly isolated or cultured neonatal or adult Schwann cells without ONA co-transplantation. Note the slightly greater difference between the slopes of the best-fit lines for freshly isolated versus cultured neonatal Schwann cells than between slopes for freshly isolated neonatal versus adult Schwann cells. **C:** Differential effects of ONA co-transplantation on remyelination by freshly isolated and cultured neonatal Schwann cells. Graph plots individual data points and best-fit lines for transplant protocols using cultured or freshly isolated neonatal Schwann cells with or without co-transplanted ONAs. Note that ONAs slightly increase total remyelination when co-transplanted with cultured Schwann cells, but decrease remyelination when co-transplanted with freshly isolated Schwann cells. **D:** Effects of prior nerve crush on remyelination. Graph of total remyelination versus lesion size for transplant experiments using freshly isolated young adult Schwann cells from normal sciatic nerves and nerves crushed 1 week prior to harvesting, with or without co-transplanted ONAs. Note that prior nerve crushes result in a small increase in remyelination, comparable to ONA co-transplantation. **E:** Relationship among lesion size, transplantation protocol, and total remyelination. Graph illustrates best-fit lines for total remyelination as a function of lesion size for the seven major classes of Schwann cell transplant protocols, and for control lesions without Schwann cell transplantation. Inset table summarizes slopes and standard errors of best-fit lines for each experimental group. Note that total remyelination increases with lesion size for all transplant protocols and that all Schwann cell transplants protocols significantly increase total remyelination compared with control lesions.

TABLE 1

Data Summary[1]

Condition	No.	% Expected dorsal column volume (k)	Maximum remyelination density (axons/mm^2)	Total remyelination ($M_{re,\ total}$) (axon * mm)	%Myelin restoration ($M_{restore}$)
Intact dorsal column	2		110,000 ± 3,000[2]		
Intact sciatic nerve	1		43,000 ± 2,000[2]		
X-EB	8	81 ± 6[3]	13,000 ± 6,000	1,400 ± 600	1.5 ± 0.5
ONA	3	102 ± 6*	19,000 ± 2,000	5,000 ± 2,000	5 ± 1
Fr Neo Sch	3	107 ± 6*	37,000 ± 1,000****,††	32,000 ± 2,000**,†††	22 ± 3*,†
Fr Neo Sch + ONA	5	101 ± 5*	33,000 ± 3,000*,†	25,000 ± 5,000*,†	16 ± 2**,††
Cult Neo Sch	10	120 ± 2*	27,000 ± 2,000*,†	15,000 ± 2,000*****,††	12 ± 2***,†
Cult Neo Sch + ONA	8	120 ± 1*	37,000 ± 6,000*,†	23,000 ± 4,000***,††	19 ± 2***,†††
Fr Ad Sch	17	95 ± 5	33,000 ± 2,000**,††	18,000 ± 2,000*****,†††	13 ± 2*****,†††
Fr Cr Ad Sch	5	104 ± 9	32,000 ± 2,000*,††	22,000 ± 5,000*,†	17 ± 3*,†
All Fr Ad Sch	22	98 ± 4*	33,000 ± 1,000**,††	19,000 ± 2,000*****,†††	14 ± 1*****,†††
Fr Ad Sch + ONA	2	96 ± 9	36,000 ± 6,000†	20,000 ± 4,000	14 ± 2†
Fr Cr Ad Sch + ONA	5	109 ± 6**	30,000 ± 4,000†	16,000 ± 4,000**	14 ± 3*,†
All Fr Ad + ONA	7	105 ± 5**	32,000 ± 3,000*,†	18,000 ± 3,000**,††	14 ± 2***,††
Cult Ad Sch	2	110 ± 5*	19,000 ± 3,000	6,000 ± 2,000	6 ± 2
Cult Ad Sch + ONA	6	91 ± 6	33,000 ± 3,000**,††	13,000 ± 2,000***,†	12 ± 1*****,††
Fr aged	5	81 ± 7	32,000 ± 3,000*,†	11,000 ± 1,000**,†	9 ± 2*
Cult aged + ONA	2	88 ± 4	34,000 ± 8,000	14,000 ± 2,000	15 ± 3
All neonatal Sch	26	116 ± 8**	32,000 ± 2,000*,††	21,000 ± 2,000*****,††††	16 ± 1*****,†††††
All adult Sch	37	99 ± 3*	32,000 ± 1,000**,††	17,000 ± 1,000*****,†††	13 ± 1*****,†††
All aged adult Sch	7	84 ± 5	33,000 ± 3,000*,††	12,000 ± 1,000****,†	10 ± 2**,†
All Sch only	45	102 ± 5*	31,000 ± 1,000*	17,000 ± 1,000*****,††	13 ± 1*****,†††††
All Sch + ONA	25	106 ± 6**	34,000 ± 2,000**	19,000 ± 2,000*****,†††	16 ± 1*****,†††
All fresh Sch	47	100 ± 3*	34,000 ± 1,000**,††	20,000 ± 1,000*****,†††	15 ± 1*****,†††
All cultured Sch	23	108 ± 8*	29,000 ± 1,000**,††	13,000 ± 1,000*****,††	13 ± 1*****,†††
All Sch transplants	70	104 ± 3*	32,000 ± 1,000*,†	19,000 ± 1,000*****,††	14.2 ± 0.8*****,†††

[1] For abbreviations, see list.

[2] Average myelinated axon density of 20 sampled regions of intact dorsal column or sciatic nerve.

[3] Differs from intact dorsal column at $P < 0.01$. All P values determined using unpaired Student's t-test.

* Differs from X-EB lesion at $P < 0.05$.

** Differs from X-EB lesion at $P < 0.01$.

*** Differs from X-EB lesion at $P < 0.001$.

**** Differs from X-EB lesion at $P < 0.0001$.

***** Differs from X-EB lesion at $P < 0.00001$.

† Differs from ONA transplant at $P < 0.05$.

†† Differs from ONA transplant at $P < 0.01$.

††† Differs from ONA transplant at $P < 0.001$.

†††† Differs from ONA transplant at $P < 0.0001$.